Microwave synthesis of FDU-1 silica with incorporated humic acid and its application for adsorption of Cd^{2+} from aqueous solutions

L.C. Cides da Silva,[1] G. Abate,[1] N. A. Oliveira,[1] M.C.A. Fantini,[2] J.C. Masini,[1] L.P. Mercuri,[3] O. Olkhovyk,[4] M. Jaroniec[4] and J. R. Matos[1]

[1]Instituto de Quimica da Universidade de São Paulo, São Paulo, SP, Brazil
[2]Instituto de Fisica da Universidade de São Paulo, São Paulo, SP, Brazil
[3]CETEC – Universidade Cruzeiro do Sul, São Paulo, SP, Brazil
[4]Department of Chemistry, Kent State University, Kent, Ohio 44240, U.S.A.

This work describes microwave synthesis of FDU-1 materials with and without humic acid. FDU-1 is cage-like ordered mesoporous silica with a face-centered cubic structure. The FDU-1 samples were prepared using poly(ethylene oxide)-poly-(butylene oxide)-poly(ethylene oxide) triblock copolymer ($EO_{39}BO_{47}EO_{39}$) as template and tetraethyl orthosilicate (TEOS) as silica source. The samples with incorporated humic acid were synthesized by using different concentrations of humic acid, i.e., 1.0, 1.5 and 2 mmoles. The resulting materials were characterized by thermogravimetry, elemental analysis, nitrogen adsorption, and small angle X-ray diffraction. The samples with incorporated humic acid were tested for removal of Cd^{2+} from aqueous solutions at pH=6. It is shown that the incorporation of humic acid into FDU-1 afforded materials with high adsorption capacity for cadmium ions. These materials seem to be promising adsorbents for removal of cadmium and related heavy metal ions from aqueous solutions.

1. INTRODUCTION

Nanoporous solids are commonly used as adsorbents, catalysts and catalyst supports due to their high surface areas. According to the IUPAC classification [1] porous materials are divided into three major groups: (i) macroporous solids, having pores of widths larger than 50 nm; (ii) mesoporous solids with pores of widths between 2 and 50 nm; and (iii) microporous solids with pores of widths below 2 nm. In 1992 a new family of mesoporous materials, designated as M41S, was reported by Mobil researchers [2]. The first ordered mesoporous silicas (OMS) such as MCM-41 [2-4], MCM-48 [2-5], FSM-16 [6] and related materials [7-11], exhibited channel-like mesoporous structures. Later, OMS with cage-like structures were obtained [7,11,12]. The FDU-1 silica is a highly ordered silica with cage-like mesoporous structure synthesized from tetraethylorthosilicate (TEOS) in the presence of poly(ethylene oxide)-poly(butylene oxide)-poly(ethylene oxide) as template. Matos *et al.* [13] showed that FDU-1 is not a cubic *Im3m* structure, as reported earlier, but a cubic *Fm3m* structure with 3-D hexagonal intergrowth, similar to SBA-2 and SBA-12. It was

demonstrated that the FDU-1 cage-like mesoporous structure can be tuned to achieve a highly open and accessible porosity with narrow pore size distribution by controlling temperature and time of the synthesis [13]. The FDU-1 samples with large adsorption capacity, remarkable hydrothermal stability and uniform pore entrances can be easily synthesized [14]. The required hydrothermal treatment can be performed in a microwave oven. Komarneni *et al.* [15,16] reported a rapid microwave-assisted synthesis of SBA-15, which offers many advantages over conventional synthesis such as a quick achievement of the crystallization temperature in the entire volume, homogeneous nucleation, a shorter crystallization time in comparison to the conventional hydrothermal process and low energy usage [17]. This method has been successfully applied for the synthesis of several types of zeolites and many ordered mesoporous materials [14,15,18]. Recently, the microwave-assisted synthesis was successfully used to obtain the FDU-1 samples [19].

Humic substances (HS) are among the most important and abundant phases of natural organic matter in soils, sediments and water. They are formed in the environment by chemical and biological decomposition of plants, roots, animals and metabolic activity of microorganisms [20,21]. Humic substances are divided into three groups according to their solubility: humic acid, which is soluble in alkali and precipitate in acidic medium; fulvic acid, which is soluble in acidic or basic media; and humin, which is insoluble in the entire pH range [20]. Due to the high content of carboxylic and phenolic groups, HS interact strongly with pollutants such as heavy metals cations and pesticides, influencing their mobility and bioavailability in the environment [20]. In addition, they are able to form aggregates with mineral particles, enhancing adsorption or complexation of heavy metal ions by these materials [22]. Thus, the understanding of the HS behavior in mineral phases has been extensively investigated nowadays [23,24], especially in terms of the removal of water contaminants. Liu and Gonzalez [24] studied the removal of Cu^{2+}, Pb^{2+} and Cd^{2+} by montmorillonite (MT) in the presence and absence of humic acid (HA). This study showed that the presence of bivalent heavy metal cations increases adsorption of HA. Also, the presence of HA enhanced adsorption of these metal ions on MT, which may form the bridge between MT and HA. Lai *et al.* [25] demonstrated that a goethite-coated sand removed Cd^{2+} efficiently above pH = 6, but at lower pH this process was almost negligible. However, the modification of this mineral phase with HA led to a significant increase in the adsorption capacity even at pH close to 2.5, which can be explained by a strong adsorption of HA on this mineral phase in acidic medium [24]. Furthermore, the removal of Cd^{2+} was more efficient by goethite-coated sand, which was initially modified with HA, than in the case of unmodified mineral exposed to a solution containing HA-complexed Cd^{2+} ions.

This paper reports the microwave synthesis of two types of the FDU-1 materials, with and without incorporated humic acid. The aforementioned materials were characterized by thermogravimetry, small angle X-ray diffraction (SAXRD) and nitrogen adsorption. The latter was used to evaluate the specific surface area, pore volume and pore size distribution of the materials studied. The performance of FDU-1 and FDU-1/HA for the removal of Cd^{2+} was assessed at pH 6, a condition that favors Cd^{2+} retention by HS and eliminates a significant contribution arising from $CdOH^{+}$ and $Cd(OH)_2$ species. This study was performed by using batch method at low Cd^{2+} concentrations, i.e., conditions that resemble solution concentrations in wastewater after primary removal of metal ions by alkaline precipitation.

2. EXPERIMENTAL

2.1. Humic acid preparation

Fifteen grams of sodium salt of HA from Aldrich were dissolved in 100 mL of 0.1 M NaOH solution under N_2 atmosphere. After 15 min the suspension was centrifuged at 1000 g for 30 min and the supernatant phase was acidified with 6 M HCl until the pH 1.0 was achieved. The suspension was centrifuged and the precipitated HA was washed with deionized water four times for the removal of salt excess. Finally, the solid phase that consisted of HA was re-suspended in 250 mL of deionized water. The HA concentration in this stock suspension was 28.0 ± 0.6 g L^{-1}, which was determined gravimetrically by drying 1.00 mL aliquots. The ash content was $(8.0 \pm 0.5)\%$, while the elemental composition of the dry HA was: $(49.7 \pm 0.1)\%$ C, $(4.3 \pm 0.1)\%$ H and $(0.65 \pm 0.02)\%$ N determined by using the elemental analyzer 2400 instrument from Perkin Elmer. To facilitate the handling of the HA suspension, and its subsequent incorporation in FDU-1, the pH of a 25.00 mL aliquot was adjusted to 7.5 using 1.0 M $NaHCO_3$ solution followed by its dilution to 50.00 mL, which gave the final HA concentration of 14.0 g L^{-1}.

2.2. FDU-1 and FDU-1/ HAx synthesis

The synthesis of the FDU-1 samples was carried out using the same synthesis gel composition as reported by Yu *et al.* [11,12]: 1 TEOS: 0.00735 B50-6600: 6 HCl: 155 H_2O, where TEOS stands for tetraethylorthosilicate from Aldrich Chemical Company, B50-6600 is a poly(ethylene oxide)-poly(butylene oxide)-poly(ethylene oxide) triblock copolymer $EO_{39}BO_{47}EO_{39}$ from Dow Chemicals. In the synthesis of FDU-1/HAx, 1.0, 1.5 and 2.0 mmoles of HA was used to obtain samples with various amount (denoted by x) of incorporated HA. In a typical synthesis procedure, 2 g of B50-6600 copolymer was dissolved in 120 g of 2 M HCl and stirred at room temperature until a homogeneous mixture was obtained. Subsequently, 8.32 g of TEOS and 22.8, 34.3 and 45.7 mL of 14 g L^{-1} HA solution, respectively, were added. The resulting mixture was stirred vigorously in an open beaker for 24 hours at room temperature. The precipitation was observed in 30 − 40 min after the addition of TEOS and HA solution. The obtained mixture was transferred into a Teflon vessel and heated under autogenous pressure for 120 min at 373 K using a microwave oven. The microwave treatment was performed using Microsynth Labstation for microwave assisted synthesis (Milestone Inc). Finally, the precipitate was filtered out, washed with 2M HCl solution and dried at 298 K. The template in as-synthesized materials was removed by soxhlet extraction at boiling point for 12 h using ethanol to yield FDU-1/HA and FDU-1. The pure silica samples are denoted as FDU-1, whereas the HA incorporated materials are denoted as FDU-1/HAx (where x = 10, 15 and 20 and it represents initial concentration of HA in the synthesis gel, respectively, 1.0, 1.5 and 2.0 mmoles)

2.3. Adsorption, thermogravimetric and X-ray diffraction measurements

Adsorption isotherms were measured on Micromeritics model ASAP 2010 volumetric adsorption analyzer (Norcross, GA) using nitrogen of 99.998% purity. Measurements were performed in the range of relative pressure from 10^{-6} to 0.995 at 77K on the samples

degassed for 2 hours at 383K under vacuum of about 10^{-3} Torr. The degassing temperature (383K) was selected to avoid the decomposition of attached organic ligands and ensure thermodesorption of physically adsorbed water.

The specific surface area was evaluated using the BET method [26]. The total pore volume was estimated from the amount adsorbed at a relative pressure of 0.99. The pore size distribution (PSD) was calculated using the BJH [27] algorithm with the relation between the capillary condensation pressure and the pore diameter established by Kruk, Jaroniec and Sayari (KJS) [28].

The thermogravimetric TG curves and differential DTG curves were obtained on a model TGA50 thermogravimetric analyzer (Shimadzu) using sample mass of ~5 mg in Pt crucible heated with heating rate of 10 K min^{-1} up to 1173 K under flowing air (50 mL/min).

The experiments SAXRD were carried out in a rotating anode X-ray generator (Rigaku), operating at 10 kW. The wavelength of the copper monochromatic X-ray beam was λ = 1.5418 Å. An image plate detector was utilized to record the scattering vector q = $(4\pi\sin\theta)/\lambda$, where θ is the half of the scattering angle. The intensity was recorded during 1 hour. The line focus geometry was used and the system was collimated by slits. A vacuum path between the sample and the detector was utilized. The scattering of the sample holder was subtracted from the total measured intensities. The sample to detector distance (~ 480 mm) was chosen to record the scattering intensity for q values ranging from 0.008 Å^{-1} to 0.35 Å^{-1}. The samples were placed inside a quartz tube, 1.5 mm in thickness.

2.4. Cadmium adsorption measurements

The pH of 10.0 g L^{-1} suspensions of FDU-1 (A) and four synthesized FDU-1/HA samples (B-E) was adjusted to 6.0 ± 0.1 with 0.1 M NaOH solution. Afterward, 5.00 mL aliquots of each suspension previously homogenized were transferred to six polypropylene centrifuge tubes (15 mL), plus 0.25 mL of the buffer, 0.1 M 2-[N-morpholino]-ethanesulfonic acid (MES, pK_a 6.15), pH 6.0. Increasing volumes of a 100 μmol L^{-1} stock Cd^{2+} solution were added to the centrifuge tubes to achieve Cd^{2+} concentrations between 0.50 and 10.0 μmol L^{-1} in total volumes of 10.0 mL. It is important to notice that the MES buffer forms only weak complexes with cadmium [25], which do not interfere with the voltammetric Cd^{2+} determination. A blank experiment was carried out in parallel to each sample. All tubes were closed and maintained under gentle shaking for 24 h. After this time the pH was checked and corrected if necessary. The tubes were centrifuged at 2600 g for 15 min, and the supernatant solutions were stored for further cadmium determination.

Determination of the equilibrium concentrations of Cd^{2+} were carried out by anodic stripping voltammetry (ASV) using a potentiostat from EG&G (Princeton, NJ, USA) coupled to a 303A model static mercury electrode also from EG&G, using a mercury drop with radius of 0.46 mm. An Ag/AgCl reference electrode and a Pt wire were used to complete the electrochemical cell. Data acquisition was performed with the model 270/250 Research Electrochemistry Software from EG&G. The mercury capillary was fitted to a flow-through cell previously described by Abate et al. [29]. The Cd^{2+} solutions were first buffered and analyzed in presence of 0.050 M sodium acetate/acetic acid buffer (pH 4.7) and 0.10 M NaNO$_3$, used as supporting electrolyte. Accumulation of Cd^0 in the Hg drop was monitored under continuous flow during 60 s of deposition time. The instrument was calibrated using five Cd^{2+} standards with concentrations between 0.05 and 1.00 μmol L^{-1}. Square wave voltammetry (SWV) was used as a technique for the potential scanning and

current sampling with the following parameters: frequency = 60 Hz, pulse height = 25 mV, deposition potential = -900 mV, deposition time = 60 s, flow rate during the deposition time = 3.5 mL min^{-1}, final potential = -100 mV. The potential scan was performed under condition of a quiescent solution. These experimental conditions provided a quantification limit of 0.02 μmol L^{-1} Cd^{2+}.

3. RESULTS AND DISCUSSION

The FDU-1 samples were isolated as solids in the form of fine powder with low density. The samples with incorporated HA showed colors that vary from light beige to brown, depending on the quantity of incorporated HA. During the extraction process of the template, a slight change in the solvent color was observed, indicating a partial removal of HA along with the template removal from the materials.
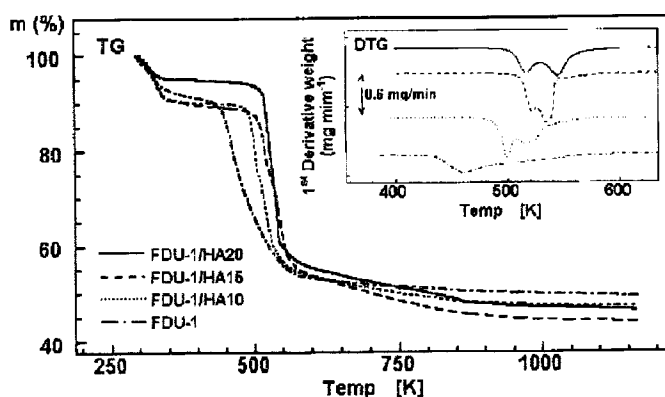

Fig. 1. TG/DTG curves for as-synthesized FDU-1 and FDU-1/HAx samples.

The TG curves for as-synthesized samples show a weight loss at about 373 K due to the liberation of physically adsorbed water (Figure 1). The thermal decomposition of the template and incorporated HA occurs between 423 and 1023 K. According to the DTG curves (inset in Figure 1), the incorporation of HA into silica structure influences the thermal decomposition of the template. The template decomposition in pure silica (FDU-1) is reflected by a wide peak on the DTG curve. In the case of the FDU-1/HAx materials this peak is shifted to higher temperatures and splits into two DTG peaks (Table 1). This effect becomes more pronounced for the materials that have larger amount of incorporated HA. Table 1 shows the weight losses (Δm_1 and Δm_2) and relative DTG peak temperatures (T_1 and T_2) for the thermal decomposition of the template and HA in as-synthesized samples.

The small angle X-ray diffraction (SAXRD) for selected solvent-extracted FDU-1 and FDU-1/HA15 samples are shown in Figure 2. The SAXRD pattern for FDU-1 features at least three reflections that can be indexed as 111, 220 and 311. The pattern for FDU-1/HA15 features at least seven reflections; the main ones can be indexed as 111, 220, 311, 400 and 420. The SAXRD patterns for these two samples were quite similar to the powder XRD patterns reported earlier for the FDU-1 structure with a face-centered cubic symmetry [13] synthesized via conventional synthesis route, i.e., using conventional oven for hydrothermal

treatment. The SAXRD patterns for the samples with incorporated 1.5 mmol of HA showed better resolved peaks.

Table 1. TG/DTG data for as-synthesized FDU-1 and FDU-1/HAx samples and nitrogen adsorption parameters for the corresponding extracted samples.

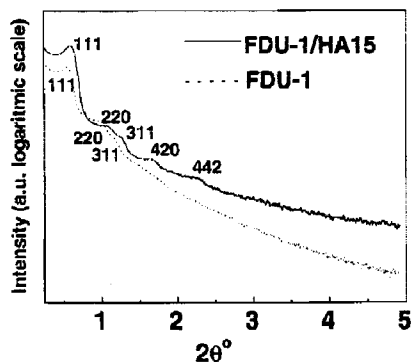| As-synthesized samples	$\Delta m_1(\%)$ (298–373K)	$\Delta m_2(\%)$ (373–1023K)	DTG Peak (K) T_1	T_2	Extracted samples	Specific surface area (m^2/g)	Pore volume (cc/g)	Pore width (nm)
FDU-1 AS	8.2	42.1	460	-	FDU-1	326	0.37	9.6
FDU-1/HA10 AS	9.7	43.0	499	517	FDU-1/HA10 EX	302	0.44	10.9
FDU-1/HA15 AS	4.9	46.1	521	535	FDU-1/HA15 EX	343	0.49	10.7
FDU-1/HA20 AS	9.7	48.1	517	544	FDU-1/HA20 EX	32	0.07	10.8

Fig. 2. Small angle X-ray diffraction patterns for the FDU-1 and FDU-1/HA15 samples.
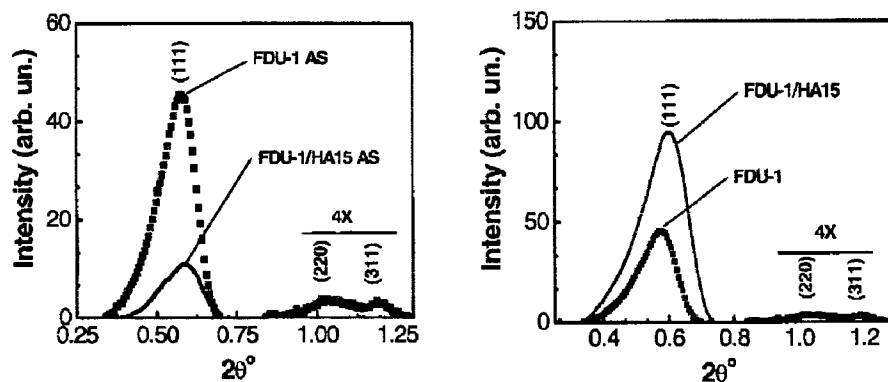

Fig. 3. Small angle X-ray diffraction patterns for as-synthesized (left panel) and extracted (right panel) FDU-1 and FDU-1/HA15 samples.

Shown in Figures 3 is a comparison of the SAXRD patterns for as-synthesized (left panel) and extracted (right panel) FDU-1 and FDU-1/HA15 samples. A small decrease in

the unit cell parameter is observed for the samples after template extraction (26.5 vs. 25.8 nm), which can be related to the structure shrinkage caused by extraction process. For as-synthesized samples with incorporated HA the diffraction intensities are smaller in comparison to FDU-1 (AS) due to the presence of HA inside pores that decreases the electronic contrast between the compound inside pores and the silica framework. However, extraction of the template resulted in the intensity increase in comparison to the corresponding as-synthesized samples, which is attributed to the increase in the electronic contrast after removal of the polymeric template from mesopores. For the samples studied the structural ordering decreased with increasing amount of incorporated HA. The worst ordering was observed for the sample with largest HA content (2.0 mmol).
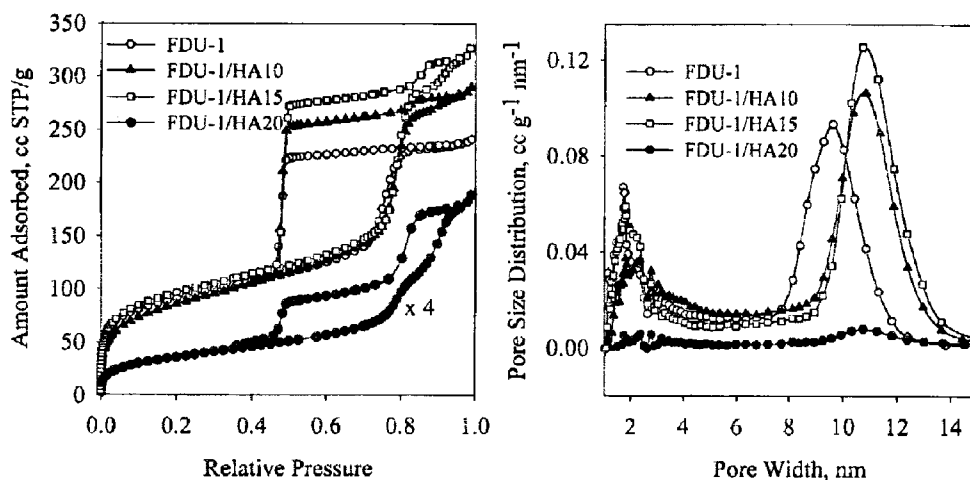

Fig. 4. Nitrogen adsorption isotherms at 77K (left panel) and the corresponding pore size distributions (right panel) for the extracted FDU-1 and FDU-1/HAx samples.

The nitrogen adsorption isotherms measured for the extracted samples feature high adsorption capacity (left panel in Figure 4). A relatively large amount of micropores is related to the interconnections between cage-like mesopores as well as to the microporosity present in the walls of mesopores. The steep capillary condensation steps at the relative pressure of ~0.8 indicate uniformity of pore sizes. A comparison of the FDU-1 samples with and without humic acid shows that an increase in the amount of the incorporated HA resulted in favorable structural changes of the samples, i.e., cause an increase in the adsorption capacity, pore volume and pore size for the FDU-1/HA15 and FDU-1/HA20 samples (Table 1). A broad hysteresis loop, which closes at a relative pressure of ~0.45, is characteristic for cage-like mesoporous materials such as FDU-1, indicating a large difference in the size of mesopores and their entrances. An increase in the amount of HA incorporated in FDU-1 up to 1.5 mmoles did not cause a noticeable change in the pore entrance size. The capillary condensation and delayed capillary evaporation steps occur at the same relative pressures for the FDU-1 samples with and without HA. A further increase in the HA amount caused almost total structure deterioration (see adsorption isotherm for FDU-1/HA20). An enlarged nitrogen adsorption isotherm for this sample shown in the left panel of Figure 4 exhibits stepwise capillary condensation and evaporation steps, which indicate poor structural ordering reflected by large non-uniformity of pore sizes and pore

entrances. Also, the adsorption capacity of this sample was only about 10-15% of that for the other samples studied.

The FDU-1 sample without HA removed only ~33% of the initial Cd^{2+} concentration (see left panel in Figure 5). The corresponding Cd^{2+} adsorption isotherm shown in the right panel of this figure is almost linear. At pH 6.0 silanols are partially deprotonated as shown by the following reaction:

$$SiOH \rightarrow SiO^- + H^+ \quad (pK_a\ 6 - 7) \tag{1}$$
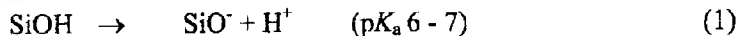
Negatively charged SiO^- groups facilitate electrostatic attraction of Cd^{2+}, which may explain the observed removal of Cd^{2+}. Due to the polarization effect, the SiO^- group behaves as a weak Lewis base, and consequenly, chemisorption of trace metals is not favorable on the silica surface [30]. Therefore, the amount of adsorbed Cd^{2+} on silica is small.

The initial pH value of all suspensions of FDU-1/HAx was near 4.4, which is favorable for adsorption of HA in comparison to pH 6 because a decrease in the pH value induces the development of positive charges on the FDU-1 surface. This delineates the mechanism of ligand exchange between carboxyl groups of HA and surface hydroxyls yielding a surface complex, which seems to be stable under constant pH and ionic strength [23]. Therefore, desorption of humic substances seems to be negligible at small pH variations, although the functional groups such as –COOH and –COH could dissociate to –COO⁻ and –CO⁻, respectively, which can cause a pH increase [25].
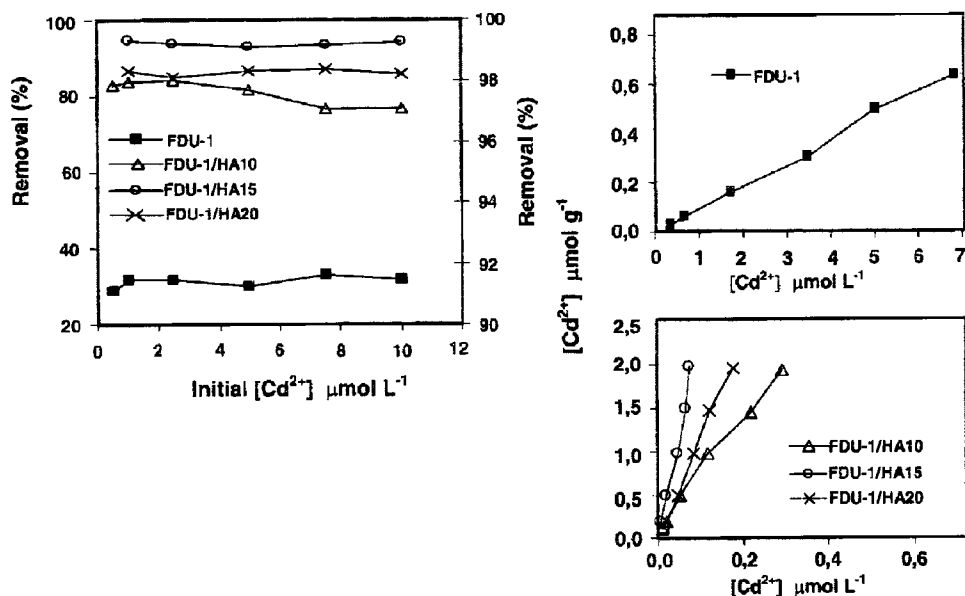

Fig. 5. The % removal of Cd^{2+} from the aqueous phase containing the FDU-1 particles at pH=6 (left panel, in which the left axis refers to FDU-1 and the right axis refers to the FDU-1/HA samples; MES = 2.5 mmol L⁻¹, equilibrium time = 24 hrs, initial [Cd^{2+}] between 0.5 and 10.0 μmol L⁻¹) and the adsorption isotherms for Cd^{2+} (right panel) corresponding to data shown in the left panel.

Figure 5 shows that the order of Cd^{2+} removal for the FDU-1/HAx samples was: FDU-1/HA15 > FDU-1/HA20 > FDU-1/HA10. It is worthy to note that even for the highest initial concentration (10 μmol L⁻¹), the remaining Cd^{2+} after the equilibrium time was only 0.073

μmol L^{-1} for the FDU-1/HA15 sample. Thus, ~99.3% of the initial Cd^{2+} was adsorbed, showing an excellent removal capacity of this adsorbent. The FDU-1/HA15 sample exhibited the highest values of the BET surface area (343 m^2/g) and pore volume (49 cc/g). Although the HA content in FDU-1/HA20 was higher than in FDU-1/HA15, the removal capacity of the former was slightly smaller. This fact may be due the partial blockage of the pores by HA as well as small surface area (32 m^2/g) and small pore volume (0.07 cc/g) of this sample in comparison to the other adsorbents studied. Also, a small desorption of HA from FDU-1/HA20 may contribute to the lower adsorption capacity of this sample. The later possibility would lead to the formation of soluble and weak Cd-HA complexes, which are easily detectable by voltametric method [29], especially at pH 4.7. In the concentration range studied, the isotherm curves shown in Figure 5 suggest the occurrence of strong adsorbent-adsorbate interactions, which are responsible for high affinity of the FDU-1/HAx adsorbents toward Cd^{2+}.

4. CONCLUSIONS

The DTG curves show that the incorporation of HA into silica structure influences the thermal decomposition of the polymeric template, which is shifted toward higher temperatures. Also, in the case of the FDU-1/HAx samples this process occurs in two steps, which are more pronounced for the samples with larger amount of incorporated HA.

The SAXRD results demonstrated that the HA incorporation does not influence the structural ordering of FDU-1 up to about 1.5 mmoles of HA. The as-synthesized and extracted FDU-1/HAx materials exhibited high structural ordering, large pores (~10 nm) and the BET surface area as high as 300 m^2/g.

The insertion of HA into mesopores of FDU-1 afforded adsorbents with excellent adsorption capacity for cadmium ions, suggesting that these materials are promising for cadmium removal from aqueous solutions. The performance of the HA-incorporated FDU-1 materials as adsorbents for other metal ions such as Hg^{2+}, Pb^{2+} and Cu^{2+} should be also remarkable because those ions show even stronger affinity to the HA binding sites than Cd^{2+}. The FDU-1/HAx adsorbents studied seem to be promising for use in wastewater treatment plants after usual alkaline precipitation.

5. ACKNOWLEDGMENT

REFERENCES

[1]   K.S.W Sing, D.H. Everett, R.A.W Haul, L. Moscou, R.A. Pierotti, J.Rouquerol, T Siemieewska, Pure Appl. Chem., 57 (1985) 603.

[2]   C.T. Kresge, M.E. Leonowicz, W.J. Roth, J.C. Vartulli, J.S. Beck, Nature, 359 (1992) 710.

[3] J.S. Beck, J.C. Vartulli, W.J. Roth, M.E. Leonowicz, C.T. Kresge, K.D. Schmitt, C.T-W. Chu, D.H. Olson, E.W. Sheppard, S.B. McCullen, J.L. Schenker, J. Am. Chem. Soc., 114 (1992) 10834.

[4] C.-Y. Chem, H.-X. Li, M.E. Davis, Micropor. Mater., 2 (1993) 17.

[5] A. Monnier, F. Schuth, Q. Huo, D. Kumar, D. Margolese, R.S. Maxwell, G.D. Stucky, M. Krishnamurty, P. Petroff, A. Firouzi, M. Janicke, B.F. Chmelka, Science, 261 (1993) 1299.

[6] S. Inagaki, Y. Fukushima, K. Kuroda, Chem. Commun., (1993) 680.

[7] Q.Huo, D.I. Margolose, U. Ciesla, P.Feng, T.E. Gier, P. Sieger, R. Leon, P.M. Petroff, F. Schuth, G.D. Stucky, Nature, 368 (1994) 317.

[8] P.T. Tanev, T.J. Pinnavaia, Science, 267 (1995) 865.

[9] R. Ryoo, J.M. Kim, C.H. Ko, C.H. Shin, J. Phys. Chem. B, 100 (1996) 17718.

[10] S. A. Bagshaw, E. Prouzet, T.J. Pinnavaia, Science, 269 (1995) 1242.

[11] D. Zhao, Q. Huo, J. Feng, B.F. Chmelka, G.D. Stucky, J. Am. Chem. Soc., 120 (1998)6024.

[12] C. Yu, B. Tian, J. Fan, G. D. Stucky, D. Zhao, J. Am. Chem. Soc., 124 (2002) 4556.

[13] J.R. Matos, M. Kruk, L.P. Mercuri, M.Jaroniec, L. Zhao, T. Kamiyama, O. Terasaki, T.J. Pinnavaia, Y. Liu, J. Am. Chem. Soc., 125 (2003) 821.

[14] J.R. Matos, L.P. Mercuri, M. Kruk, M. Jaroniec, Langmuir, 18 (2002) 884.

[15] S. Komarneni, D. Li, L.N. Bharat, H. Katsuki, A.S. Bhalla, Langmuir, 18 (2001) 5959.

[16] L.N. Bharat, J. Olanrewaju, S. Komarneni, Chem. Mater., 13 (2001) 552.

[17] C. Gabriel, S. Gabriel, E. H. Grant, B. S. J. Halstead, D. M. P. Mingos, Chem. Soc. Rev., 27 (1998) 213.

[18] H. Katsuki, S. Furuta, S. Komarneni, Journal of Porous Mater., 8 (2001) 5.

[19] M.A.C. Fantini, J.R. Matos, L.C. Cides da Silva, L.P. Mercuri, G.O. Chiereci, E. Celer, M. Jaroniec, J. Eng. Sci. Mat. B., 112 (2004) 106.

[20] F.J. Stevenson, 1994. Humus Chemistry. Genesis, Composition, Reactions, Willey Interscience, New York.

[21] M.H.B. Hayes, C.E. Clapp, Soil Science, 166 (2001) 723-737.

[22] D. Buerge-Weirich, R. Hari, H. Xue, P. Behra, L. Sigg, Environ. Sci. Technol., 36 (2002) 328-336.

[23] E.M. Murphy, J.M. Zachara, Geoderma, 67 (1995) 103-124.

[24] G. Abate, J.C. Masini, Coll. Surf. A: Physicochem. Eng. Asp., 226 (2003) 25-34.

[25] C. Lai, C.Chen, B. Wei, S. Yeh, Water Research, 36 (2002) 4943-4950.

[26] S. Brunauer, P.H. Emmett, E.Teller, J. Am. Chem. Soc., 60 (1938) 309.

[27] E. P. Barrett, L. G. Joyner, P. H. Halenda, J. Am. Chem. Soc., 73 (1951) 373.

[28] M. Kruk, M. Jaroniec, A. Sayari, Langmuir, 13 (1997) 6267.

[29] G. Abate, J.C. Masini, Organic Geochem., 33 (2002a) 1171-1182.

[30] M.B. Mc Bride, 1994. Environmental Chemistry of Soils, Oxford University Press.

[31] A. Liu, R.D. Gonzalez, J. Coll. Interf. Sci., 218 (1999) 225-232.